Energy Wheel Performance and Optimization Opportunities for SDVAV AHU's In a Hot & Humid Climate

J. Zhao[1], L. Wang[2], and J. Watt[3]

[1] *Research Engineering Associate IV (Ph.D, PE), Energy Systems Laboratory, Texas A&M University, 402 Harvey Mitchell Pkwy, College Station, Texas 77845*
[2] *Research Engineering Associate III (Ph.D, PE), Energy Systems Laboratory, Texas A&M University, 402 Harvey Mitchell Pkwy, College Station, Texas 77845*
[3] *Senior Research Engineer (PE), Energy Systems Laboratory, Texas A&M University, 402 Harvey Mitchell Pkwy, College Station, Texas 77845*

Email: juanzhao@tees.tamus.edu

Abstract:

The HVAC system accounts for 30 to 50 percent of a typical building's energy consumption; in hot & humid climates it is closer to the upper end of that range. Implementing effective energy saving measures for the building HVAC system can reduce the building energy consumption, reduce peak demand, and improve building comfort. The energy wheel is widely used in new system designs to recover/reject both sensible and latent heat energy from/to the exhaust airflow of air handling units. In this study, field measurements were conducted to evaluate the performance of one energy wheel installed in a SDVAV AHU serving an education building on a large university campus located in a hot and humid area. This paper also presents recommended optimization and performance improvement opportunities associated with this unit based on the performance evaluation.

Keywords:

Air handling unit, Energy efficiency, Energy wheel, Performance Improvement

1. Introduction

The air-to-air rotary energy wheel, as a widely-used energy recovery unit, is used in building HVAC system to recover/reject both sensible and latent heat energy from/to the exhaust airflow of air handling units. The air-permeable medium filled in the revolving cylinder of the energy wheel provides large heat and mass transfer area to make the rotary energy wheel has the potential to obtain high sensible and latent heat recovery effectiveness. The advantages for applying the energy wheel as an energy recovery unit include: (1) simultaneous heat and mass transfer, (2) low pressure drop, (3) compact size, and (4) available to all ventilation system platforms; the limitations of the energy wheel application include: (1) further cooling/heating required for supply air, (2) possible cross-contamination, and (3) increased maintenance requirement under cold climate (ASHRAE, 2005).

Field testing helps to increase the confidence in energy wheel performance and promote the application of such energy-recovery devices (Zhai, et al., 2006). ASHRAE Standard 84-1991 provides guidance for laboratory testing for air-to-air enthalpy exchangers. As the enthalpy exchanger performance in the field may differ from lab application, using ASHRAE Standard 84-1991 for field performance testing is not as applicable as it is to the laboratory testing. In winter 2006, a field testing and a lab testing were performed on the enthalpy recovery wheel installed in the ventilation system of Carnegie Mellon University's Intelligent Workplace (Zhai, et al., 2006). The testing used manufactured installed instruments as well as temperature and humidity data loggers. The results show that the field testing performance matched the lab testing. The manufacture-installed sensors show 27 % discrepancy between the heat loss and heat gain. This discrepancy was reduced after implementing the purge flow to the heat balance calculation. Meanwhile, complicated heat and mass transfer equations or numerical models were developed to predict the enthalpy wheel performance. For example, Klein (Klein, et al., 1990) developed a ε-NTU model for the silica gel enthalpy wheel. Simonson and Besant (Simonson, et al., 1997) used the finite volume method (FVM) to develop a numerical model for the enthalpy wheel. Beccali (Beccali, et al., 2003) and Freund (Freund, et al., 2003) proposed simpler models for predicting the correlation for sensible, latent and total effectiveness of enthalpy wheels, but these models were still complicated and had some deficiencies; for instance in Freund model, manufacture's effectiveness data were used for determining the correction factors. Knowing that manufactures usually provide performance data for standard operating rates, Freund's model would be complicated for non-standard performance conditions. Jeong and Mumma (Jeong, et al., 2005) developed simpler method to provide reliable enthalpy wheel effectiveness correlations readily applicable to design and analysis of enthalpy wheel applications. In their research the 2^k factorial experiment design method is applied to analyze the enthalpy wheel effectiveness correlations for six variables: incoming outdoor air (OA) temperature and relative humidity, exhaust air (EA) temperature and relative humidity, face velocity and EA to OA flow ratio. In total 2^6(64) experiments on silica gel and molecular sieve enthalpy wheels were performed for the full factorial experiment. A. S. Al-Ghamdi (Al-Ghamdi, 2006) developed numerical models to study the effect of some parameters such as rotational speed, number of transfer unit, heat capacity ratio, porosity and volume flow rate on wheel effectiveness during summer and winter operations.

The performance of a rotary energy wheel is evaluated by the wheel effectiveness (e.g., sensible/latent/total effectiveness) and the wheel medium pressure drop. Under different weather conditions (e.g, dry and cold condition, humid and hot condition), the energy wheel is used for humidification or dehumidification besides of recovering sensible heat. This study focuses on an energy wheel installed in a single duct VAV air handling unit and operated under a hot and humid weather. The real-time trending data were used to estimate the wheel effectiveness. The purpose of this study is to use field data to evaluate an energy wheel performance in a hot and humid climate and identify potential performance improvement opportunities based on current operation sequence for future CC® services.

2. Case Study and Method

2.1. Study Site and Device Introduction

The study building locates on a large campus and contains offices, lecture halls, laboratories, and conference rooms. Local climate is subtropical and temperate. It is hot and humid in summer season. The air handling unit, installed with the studied energy wheel, services the lab areas of the building. Figure 1 shows the schematic diagram of the studied AHU. The part of return air re-enters service area through a by-pass damper installed between supply duct and exhaust duct. The trending data shows the supply air flow is about 3 times of the exhaust air flow. According to current operation sequence, the energy wheel operates when outside air (OA) dry-bulb temperature is less than 50 ^{o}F or greater than 60 ^{o}F. The energy wheel has VFD installed; the VFD speed is controlled based on OA dry-bulb temperature (Table 1). The design information of the energy wheel is listed in Table 2.

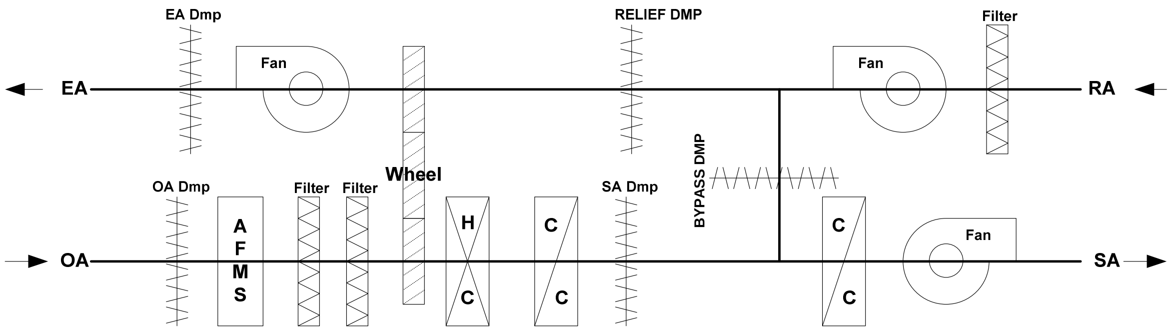

Fig. 1. Schematic diagram of AHU with studied energy wheel installed

Table 1: Energy wheel speed control sequence

OAT, ^{o}F	35	50	70	85
Wheel VFD SPD, %	100	20	20	100

Table 2: Mechanical schedule of the energy wheel

Supply Air				Exhaust Air			Total Eff.	Motor HP	Vol/PH/HZ	RPM
CFM	EAT DB/WB	LAT DB/WB	Wheel "H_2O	CFM	EAT DB/WB	Wheel "H_2O				
8,000	97/80	84.1/70.8	0.9	5,125	76.5/64	0.9	95 %	1.0	460/3/60	1725

2.2. Field Measurement Instruments and Method

The field measurements were taken for (1) entering air temperature/relative humidity and leaving air temperature/relative humidity of the energy wheel in supply side and exhaust side, (2) pressure drop of the energy wheel at different VFD speeds, and (3) air flow rate in supply side and exhaust side. Instruments used for taking these measurements include Fluke thermometer and VELOCICALC multi-function ventilation meter (Figure 2). The measurements were taken in the mixing chamber before and after the energy wheel. During measurements, the supply fan and the exhaust fan VFD drives were manually locked to maintain constant supply and exhaust air flow. Meanwhile, the energy wheel VFD was controlled to be different speed (e.g., 20 %, 60 %, 80 %, and 100 %) to take the measurements. The measurements were taken at the same time range to avoid fluctuation of supply side entering air temperature and exhaust side entering air temperature.

Fig. 2. Fluke thermometer (left) and VELOCICAL multi-function ventilation meter (right)

Besides of field measurements, HoBo data loggers were installed in the mixing chambers before and after the energy wheel to trend real-time (every 5 minutes) air dry-bulb temperature and relative humidity of supply and exhaust air stream for one week. The energy wheel speed, supply air flow and exhaust air flow were trended using the sensors installed in AHU through Siemens Apogee control system. The field measurements were taken to verify these sensors to ensure the accuracy of the trending data.

2.3. Energy Wheel Effectiveness Calculation

ASHRAE Standard 84 defines energy wheel effectiveness as:
$\varepsilon = \frac{Actural\ transfer\ of\ moisture\ or\ energy}{Maximum\ possible\ transfer\ between\ airstreams}$. (ASHRAE Handbook, 2008) According to energy transfer process, effectiveness is given as sensible effectiveness (the sensible heat transfer process), latent effectiveness (the moisture transfer process), and total effectiveness (total energy transfer including sensible heat transfer and moisture transfer). In this study, three effectiveness values were calculated based on the trending data. Figure 3 shows a schematic diagram of counter-flow airstreams through energy wheel.

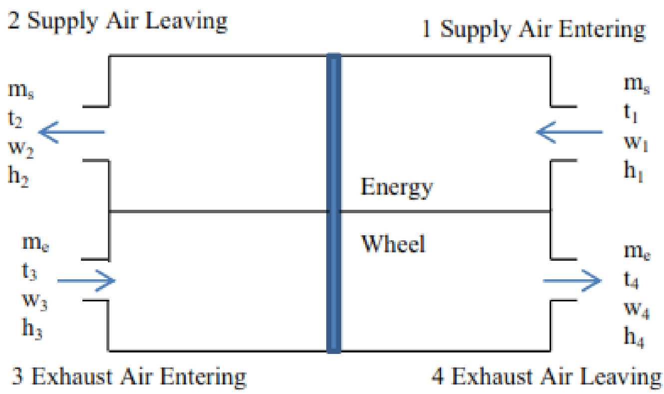

Fig. 3. Schematic diagram of counter-flow airstreams through energy wheel

The sensible effectiveness is calculated using Equation (1). This equation is applicable under the conditions: (1) no heat or moisture transfer between the wheel and surrounding, (2) no cross-leakage, (3) no energy gains from motors, fans, or front control devices.

$$\varepsilon_s = \frac{q_s}{q_{s,max}} = \frac{m_s c_{ps}(t_2 - t_1)}{C_{min}(t_3 - t_2)} = \frac{m_e c_{pe}(t_3 - t_4)}{C_{min}(t_3 - t_1)} \quad (1)$$

Where

t_1, t_2, t_3, t_4 = dry-bulb temperature at locations 1, 2, 3, and 4 in Figure 3, °F
m_s, m_e = supply and exhaust dry air mass flow rate, lb/min
C_{min} = smaller of $c_{ps}m_s$ and $c_{pe}m_e$
c_{ps}, c_{pe} = supply/exhaust moist air specific heat at constant pressure, But/lb.°F

The latent effectiveness is calculated using Equation (2).

$$\varepsilon_L = \frac{m_s(w_1 - w_2)}{m_{min}(w_1 - w_3)} = \frac{m_e(w_4 - w_3)}{m_{min}(w_1 - w_3)} \quad (2)$$

Where

w_1, w_2, w_3, w_4 = humidity ratio at locations 1, 2, 3, and 4 in Figure 3
m_{min} = smaller of m_s and m_e

The total effectiveness is calculated using Equation (3).

$$\varepsilon_t = \frac{m_s(h_1 - h_2)}{m_{min}(h_1 - h_3)} = \frac{m_e(h_4 - h_3)}{m_{min}(h_1 - h_3)} \quad (3)$$

Where

h_1, h_2, h_3, h_4 = enthalpy at locations 1, 2, 3, and 4 in Figure 3, Btu/lb

3. Results

24 hr data logger trending data in a hot and humid day was used to calculate sensible effectiveness, latent effectiveness, and total effectiveness of the energy wheel. The calculated total effectiveness of the wheel under the hot and humid weather was about 80 %, which is lower than the design value (95 %). Following plots (Figure 4 to Figure 6) show the calculated sensible/latent/total effectiveness of the energy wheel and relationship between the wheel effectiveness and OA dry-bulb temperature/humidity/wheel speed.

3.1. Energy Wheel Effectiveness vs. OA Dry-Bulb Temperature

Figure 14 shows lower (comparing to the effectiveness values when OA dry-bulb temperature is much higher than the exhaust entering temperature: space temperature- 74 ^{o}F) wheel effectiveness (sensible/latent/total) when OA dry-bulb temperature is closed to the exhaust entering temperature (space temperature). It seems, from trending data, the significant influence is on the wheel sensible effectiveness. However, the potential influence of trending data accuracy on the sensible effectiveness calculation should be considered for this OA temperature range. On the other hand, this observation shows the performance of an energy wheel at this OA temperature range may be declined.

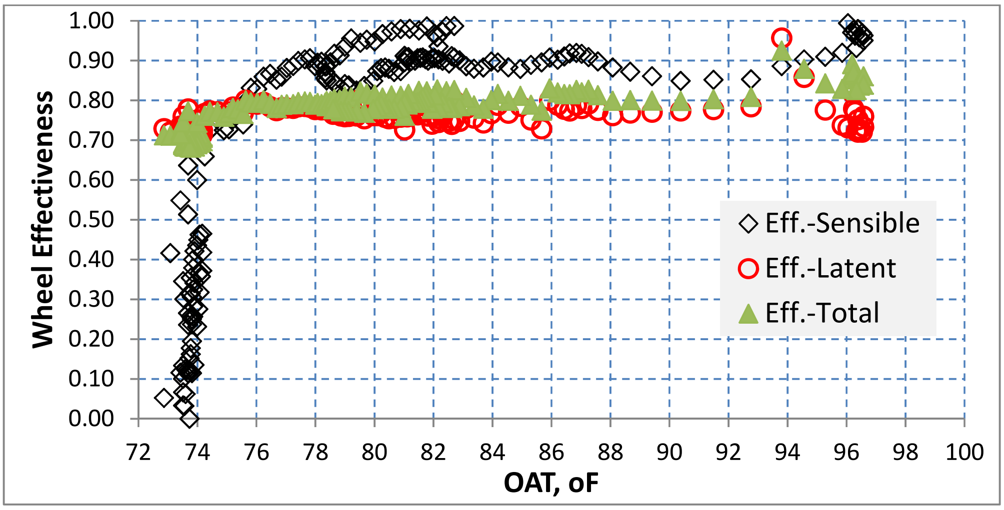

Fig. 4. Wheel effectiveness vs. OA dry-bulb temperature

3.2. Energy Wheel Effectiveness vs. OA Humidity (Dew Point Temperature)

Figure 5 shows the wheel works more efficient (average 80 % total/latent effectiveness, average 90 % sensible effectiveness) at high OA humidity condition comparing to lower humidity condition (average 70 % total/latent effectiveness, average 50 % sensible effectiveness).

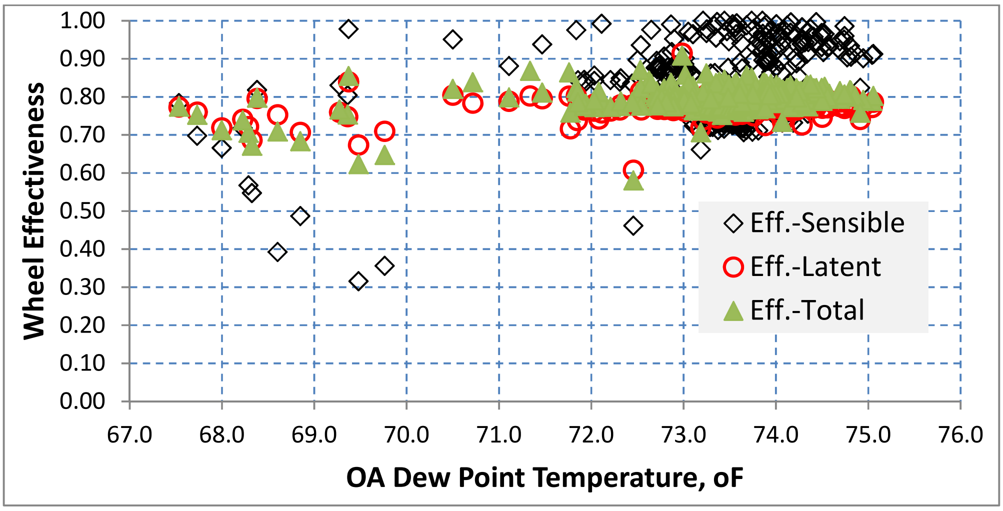

Fig. 5. Wheel effectiveness vs. OA dew point temperature

3.3. Wheel Effectiveness vs. Wheel VFD Speed

It shows in Figure 6 that the wheel effectiveness has small improvement when the wheel VFD speed is above 90 %. However, the wheel VFD speed effect on the wheel effectiveness is not significant.

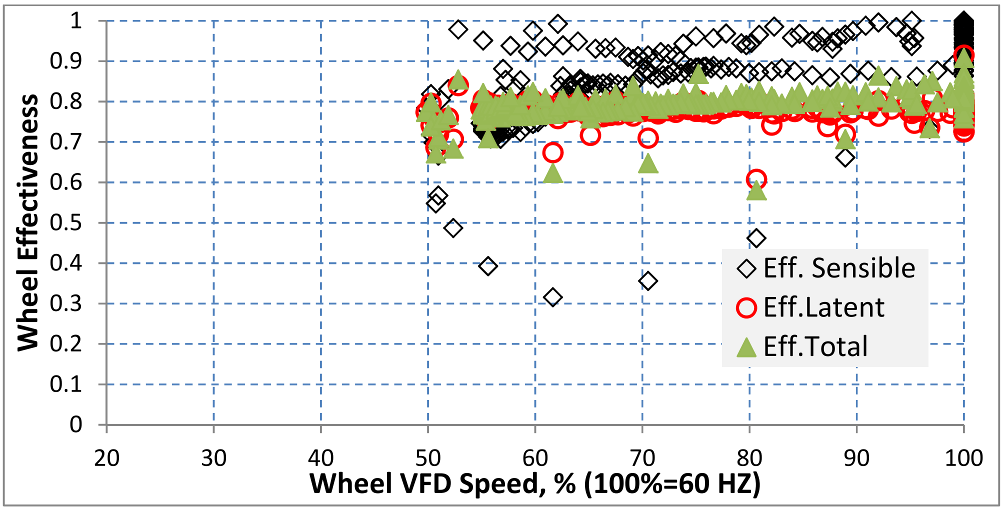

Fig. 6. Wheel effectiveness vs. wheel VFD speed

3.4. Field Estimation of Power Recovery of the AHU Installed with Studied Energy Wheel at Different Wheel Speeds

Besides of data logger trending data, field measurements were conducted to estimate power recovery from the energy wheel operation and power consumption from the energy wheel and supply fan power used to overcome pressure drop through the wheel. During measurements, the

VFDs of the supply fan and the exhaust fan were overridden to maintain fixed supply air flow (7,650 cfm) and exhaust air flow (4,207 cfm). And, the measurements were taken at the same time range to avoid fluctuation of supply side entering air temperature and exhaust side entering air temperature. The wheel VFD speed was controlled to be at 20 %, 60 %, 80 %, and 100 % respectively. Table 3 shows the calculated results, which show higher power recovery at high wheel speed. Meanwhile, the pressure drop is similar for each wheel speed.

Table 3: AHU power recovery at different wheel speeds

WHL SPD, %	Wheel Pressure Drop, inch WC	WHL electrical power consumption, kw	Wheel power recovery, kw	Supply fan power consumption, kw	Net power recovery, kw
20	0.65	(0.0039)	48.58	(16.29)	32.28
60	0.62	(0.168)	45.42	(15.94)	29.31
80	0.57	(0.434)	63.03	(13.03)	49.57
100	0.64	(0.746)	67.8	(16.39)	50.67

4. Summary and Recommendations

4.1. Summary

This study uses real-time trending data collected in a hot and humid day to estimate the sensible/latent/total effectiveness of an energy wheel installed in a single duct VAV air handling unit with the configuration in Figure 1. Meanwhile, the field measurements were conducted to estimate power recovery of the AHU for different wheel speeds. The operation performance of the studied energy wheel in a hot and humid climate is summarized as follows:

- The total effectiveness obtained from trending data is lower than the design value (80 % vs. 95 %).
- The performance of the wheel declines when OA dry-bulb temperature is closed to space temperature (exhaust air entering temperature).
- The wheel speed has not significant influence on the studied wheel effectiveness.
- The application of the energy wheel under hot and humid weather recovers energy.

This study focuses on an air-to-air rotary energy wheel installed in a single duct VAV AHU to do a preliminary evaluation of the performance of the wheel operating in a hot and humid climate. The real-time trending data and field measured data were taken when the unit operated normally. The results of this study show the performance of the studied energy wheel in its practical use. The extended studies will be needed to verify whether the performance observations from this study are applicable to other energy wheels installed in the AHUs with different configurations.

4.2. Recommendations

Based on the review of current wheel operation sequence and preliminary performance evaluation, the recommended energy wheel performance improvement opportunities are as follows:

- The by-pass damper in supply side of the AHU with the energy wheel installed should be available to implement economizer mode when the wheel is off.
- The OA dry-bulb temperature based wheel speed control should be optimized according to weather condition.

References:

Al-Ghamdi, A. S. 2006. Analysis of air-to-air rotary energy wheels, PhD Dissertation.

ASHARE. 2008. ASHARE Handbook: HVAC Systems and Equipment. American Society of Heating, Refrigerating and Air-Conditioning Engineers, Inc. Atlanta, GA.

ASHRAE. 2005. Principles of Heating, Ventilating, and Air Conditioning. American Society of Heating, Refrigerating and Air-Conditioning Engineers, Inc. Atlanta, GA.

Beccali, M., Butera, F., Guanella, R., and Adhikari, R.S. 2003. Simplified models for the performance evaluation of desiccant wheel dehumidification, International Journal of Energy Research 27(1): 17-29.

Freund, S., Klein, S.A., and Reindl, D.T. 2003. A semi-empirical method to estimate enthalpy exchanger performance and a comparison of alternative frost control strategies, HVAC&R Research 9(4): 493-508.

Jeong, J. and Mumma, S. A. 2005. Practical thermal performance correlations for molecular sieve and silica gel loaded enthalpy wheels. Applied Thermal Engineering 25(5-6): 719-740.

Klein, H., Klein, S.A., and Mitchell, J.W. 1990. Analysis of regenerative enthalpy exchangers, International Journal of Heat and Mass Transfer 33(4): 735-744.

Simonson, C.J. and Besant, R.W. 1997. Heat and moisture transfer in desiccant coated rotary energy exchangers: Part I. Numerical model, HVAC&R Research 3(4): 325-350.

Zhai, C., Archer, D.H., and Fischer, J.C. 2006. The performance of an enthalpy recovery wheel in ventilation of CMU's IW. 2006 ASME International Mechanical Engineering Congress and Exposition. Chicago, Illinois.